$CpFe(CO)_2$ Radical Generated from Dinuclear $[CpFe(CO)_2]_2$ and Mononuclear $(Cp)(CO)_2Fe(H)$: Density Functional Theory is Accurate for One, but Not Both

Kevin P. Quirion,[a] Roushan Prakash Singh,[b] Neal P. Mankad,[b] and Daniel H. Ess*[a]

[a] Department of Chemistry and Biochemistry, Brigham Young University, Provo, UT 84604, USA
[b] Department of Chemistry, University of Illinois, Chicago, IL 60607, USA

Abstract

Density functional theory (DFT) methods remain the most practical approach to calculating properties and reaction mechanisms of transition metal complexes. While the accuracy of DFT methods has been evaluated for some properties of mononuclear organometallic complexes there has been a general lack of evaluation for dinuclear organometallic complexes, in particular bonding changes related to reaction mechanisms. This work evaluated DFT and coupled cluster methods for the accuracy of calculating $CpFe(CO)_2$ radical (Fp•) generated from dinuclear $[CpFe(CO)_2]_2$ (Fp_2) and mononuclear $[(Cp)(CO)_2Fe(H)]$ (Fp-H). This transition metal radical fragment was evaluated because dinuclear complexes built with it have recently shown a variety of unique reactions but has proven challenging to accurately calculate with DFT methods. Here we show that DFT methods provide a surprising wide range of fragmentation energies for Fp_2 and lower and mid rung DFT methods as well as DLPNO-CCSD(T) perform well for this dissociation energy. The highest rung double-hybrid methods also have a large range in Fp_2 dissociation energies, and the energy greatly depends on the amount of MP2 correlation energy included. For generating Fp• from Fp-H the lower and mid rung methods that worked well for Fp_2 showed significant error. Double-hybrid methods unfortunately are only accurate for the Fe-H bond if they are very inaccurate for the Fp_2 dissociation energy. While DLPNO-CCSD(T) is not perfect, and not close to chemically accurate for the Fe-H bond, it does provide reasonable accuracy for both Fp_2 and Fp-H dissociation energies.

Introduction

Due to the balance of speed and computational cost, density functional theory (DFT) remains the most practical approach to calculating properties and reaction mechanisms of transition metal complexes. For mononuclear transition metal systems there has been some evaluation of the accuracy of DFT methods, and emergence of high and low performing density functionals generally fit within the so-called Jacob's ladder hierarchy.[1-3] In contrast to mononuclear systems,[4-6] there has not been extensive accuracy assessment of DFT methods for dinuclear complexes featuring two metal centers and properties related to bonding changes in reaction mechanisms. Evaluation of the accuracy of dinuclear complexes is important because they often have different physical properties, reactivity, and selectivity compared to mononuclear complexes.[7-9] Moreover, while our groups have used DFT methods to model a variety of dinuclear catalyzed reactions ranging from cyclization reactions to cross-coupling reactions[10-12] we generally had to resort to surveying a variety of density functionals and make a less than fully evaluated choice of functionals to interpret structures and energies.

A specific recent example where it was complicated to select a DFT method and have confidence in its accuracy was for reactions of dinuclear Fe-Al complexes with small molecules (e.g. CO_2), which occur through a reaction mechanism involving Fe and Al radicals generated through bond homolysis. Therefore, we wanted to evaluate the accuracy of DFT methods for treating dinuclear complexes where there is fragmentation to mononuclear radicals. This prompted the evaluation of DFT methods for the accuracy of calculating the $CpFe(CO)_2$ radical (Fp•) generated from dinuclear $[CpFe(CO)_2]_2$ (Fp_2)[13] and mononuclear $[(Cp)(CO)_2Fe(H)]$ (Fp-H),[14] and both of these fragmentation reactions have experimentally measured energies. Here we show that DFT methods provide a surprising wide range of fragmentation energies for Fp_2 and lower and mid rung DFT methods as well as DLPNO-CCSD(T) perform well for this fragmentation energy. The highest rung double-hybrid methods also have a large range in Fp_2 fragmentation energies, and the energy greatly depends on the amount of MP2 correlation energy

included. Fp-H bond homolysis also leads to Fp•. Surprisingly, the lower rung methods that worked well for the Fp_2 fragmentation energy showed significant error for the Fe-H bond energy. Double-hybrid methods unfortunately are only accurate for the Fe-H bond if they are very inaccurate for the Fp_2 fragmentation energy. While DLPNO-CCSD(T) does not provide chemical accuracy (i.e. within 1 kcal/mol), it does provide reasonable accuracy for both dinuclear and mononuclear fragmentation energies. Overall, this work indicates that for care should be taken when selecting a DFT method appropriate for metal radicals that toggle between dinuclear and mononuclear structures since accuracy may not readily translate from one structure to another.

Computational Methods

DFT calculations with an ultrafine integration grid were conducted using Gaussian 16[15] with the PBE0 hybrid functional labeled as PBE1PBE.[16, 17] Geometries were optimized with the def2-TZVP[18] basis set and dispersion was incorporated into PBE0 calculations using Grimme's D3 dispersion[19] correction along with the Becke-Johnson[20] (BJ) damping function. For Fp_2, the influence of solvent was evaluated by optimizing geometries in the presence of explicit benzene solvent, and for Fp-H in the presence of explicit acetonitrile solvent. Both structures also had geometries optimized using the SMD[21] continuum solvation model in their respective solvents. Vibrational frequency analysis verified all stationary points as minima and was used to calculate the thermochemical corrections at 298 K. Additional DFT single point calculations (e.g. M06-L[22]) were also carried out in Gaussian or ORCA on the PBE0 gas-phase geometries. PBE0 thermochemical corrections were then added to the additional single point energies. Several double-hybrid density functional theory (DH-DFT) methods were examined (see SI), and here we focus on the PBE0DH[23] functional. The PBE0 thermochemical corrections were applied to the DH-DFT electronic energies. Coupled cluster single point energies were calculated using PBE0 gas-phase geometries using the ORCA 6.0 software[24] with both CCSD(T)[25] and DLPNO-CCSD(T)[26] and with the def2-TZVP basis set in the gas phase. DLPNO calculations were run with TightPNO to enforce stricter cutoffs for PNOs. PBE0 thermochemical corrections were applied to these coupled cluster energies. The Nudged elastic band (NEB) calculation was conducted using the ORCA 6.0 software with the M06-L functional and the def2-SVP basis set. Subsequent single point energy calculations were conducted at each point located along the minimum energy pathway with broken symmetry spin unrestricted M06-L/def2-TZVP and the DEFGRID3 integration grid. Intrinsic bond orbitals (IBOs) were generated via IboView v20211019-RevA using the DFJX-RKS SCF method with the PBE functional, an orbital basis set of def2-TZVP, and a fit basis of univ-JFIT.[27, 28]

Results and Discussion

As has been known for multiple decades, DFT methods offer a balance between accuracy and computational cost.[29] Because of this balance, DFT methods remain the most practical method for evaluating reaction mechanisms featuring transition metal complexes, especially when evaluating reaction mechanisms where hundreds or more structures must be evaluated. There are now dozens of density functionals to choose from when modeling transition metal systems and carefully choosing which to use is highly important when dealing with electronically complex systems such as transition metal complexes.[30, 31] As outlined in the introduction, we have recently struggled to identify DFT methods that can accurately calculate the energies of mononuclear transition metal radical fragments that are generated from dinuclear starting complexes (e.g. Fe-Al complexes).[32] This prompted us to examine the accuracy of DFT methods towards the enthalpy of Fp_2 fragmentation that gives Fp•.[33-36] Fp_2 is advantageous to analyze because it has a low spin singlet ground state without any significant multireference character. We also analyzed the related Fe-H bond because it also gives the Fp•,[14, 37, 38] but starting from a mononuclear complex.

The solid state x-ray structures for Fp_2 have been reported for both the *cis* and *trans* configurations.[39-42] In solution, based on ^{13}C nuclear magnetic resonance experiments, the Fp_2 dimer is known to be fluxional with rapid interconversion between *cis*, *trans*, and open configurations (Figure 1),[43] and the *cis* is the major configuration. Here we represent only the open configuration with a Fe-Fe bond

because extended Huckel calculations by Hoffmann and our own moleulcar orbital calculations show that there is minimal direct Fe-Fe bonding in the fully optimized *cis* and *trans* geometries. See later discussion for what occurs as *cis* and *trans* Fp_2 undergoes fragmentation.

Because we previously used the PBE0 functional to evaluate Fe-Al dinuclear complexes we wanted to first assess this functional for the Fp_2 geometry and fragmentation energy to Fp•. For the geometry comparison we optimized the Fp_2 structures in the gas phase and compared them to the x-ray structures. With the PBE0 functional the key Fe-to-Fe distances (*cis*/*trans*: 2.51 Å, and open: 2.66 Å) and non-bridging Fe-C(O) distances (*cis*/*trans*: 1.75 Å, and open: 1.74 Å) are very close to the x-ray structure distances (Figure 1). The SI provides a detailed comparison showing that in general hybrid and meta hybrid DFT methods provide reasonable geometries. However, optimization of the Fp_2 geometry with the double-hybrid PBE0DH functional resulted in a Fe-to-Fe distance of 2.47 Å, which is 0.06 Å shorter than the x-ray structure. In general, the bond distances of small molecules in the gas phase and in implicit solvation will not vary significantly from that of their known crystal structures,[44] and this large of deviation is potentially significant.

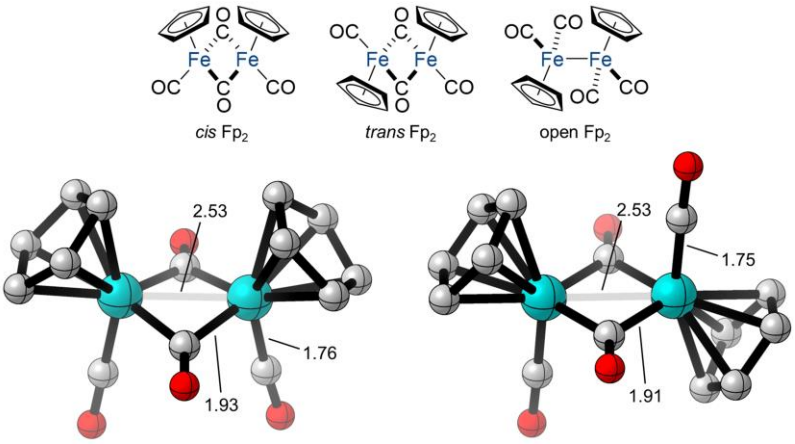

Figure 1. Top: Illustration of *cis*, *trans*, and open Fp_2 configurations. Bottom: X-ray structures[39, 41] of *cis* and *trans* configurations with key distances shown (Å).

With accurate replication of experimental geometries for Fp_2, we assumed that PBE0 would provide accurate relative energies for the configurations of Fp_2 and fragmentation to Fp•. Somewhat consistent with experiment, the PBE0 functional gave a very small energy difference between *cis* and *trans* configurations (Figure 2a). The enthalpy difference is 0.3 kcal/mol but gives the *trans* to be lower in energy than the *cis*. The open configuration with PBE0 is 3.1 kcal/mol higher in enthalpy than the *trans* geometry. All DFT methods gave the *trans* configuration to be lower in energy than the *cis* configuration. In contrast, DLPNO-CCSD(T) gave the *cis* configuration to be 0.8 kcal/mol lower in energy than the *trans* configuration and 1.7 kcal/mol lower than the open configuration.

Cutler et al. experimentally measured the Fp_2 fragmentation energy (we have avoided calling it a bond dissociation energy because of the lack of direct Fe-Fe bond in *cis* and *trans* ground state configurations), which we interpret as enthalpy, to be 26.9 kcal/mol ± 2.7 kcal/mol.[13] This value was obtained by analysis of the reaction kinetics of disproportionation of the mono acetylated species, which formed Fp_2 and the diacetylated dimer in benzene solution from 60-100 °C, and was shown to follow first order kinetics. Because this is a kinetic value and likely an upper limit of the fragmentation enthalpy, we carried out a nudged elastic band (NEB) calculation with respect to the Fe-Fe distance to determine if there is any potential energy barrier. The NEB pathway shown in Figure 3 provides energy versus Fe-Fe distance from 2.66 Å to 5.45 Å and shows that after 3.5 Å the electronic configuration has an open-shell singlet configuration. More importantly, the energy surface is very flat with a maximum energy of 27.1 kcal/mol compared to the open Fp_2 isomer (Figure 3). This means that any enthalpy barrier is within error

range of the experimental kinetic fragmentation and therefore, we have taken this kinetic value to be equivalent to the thermodynamic value.

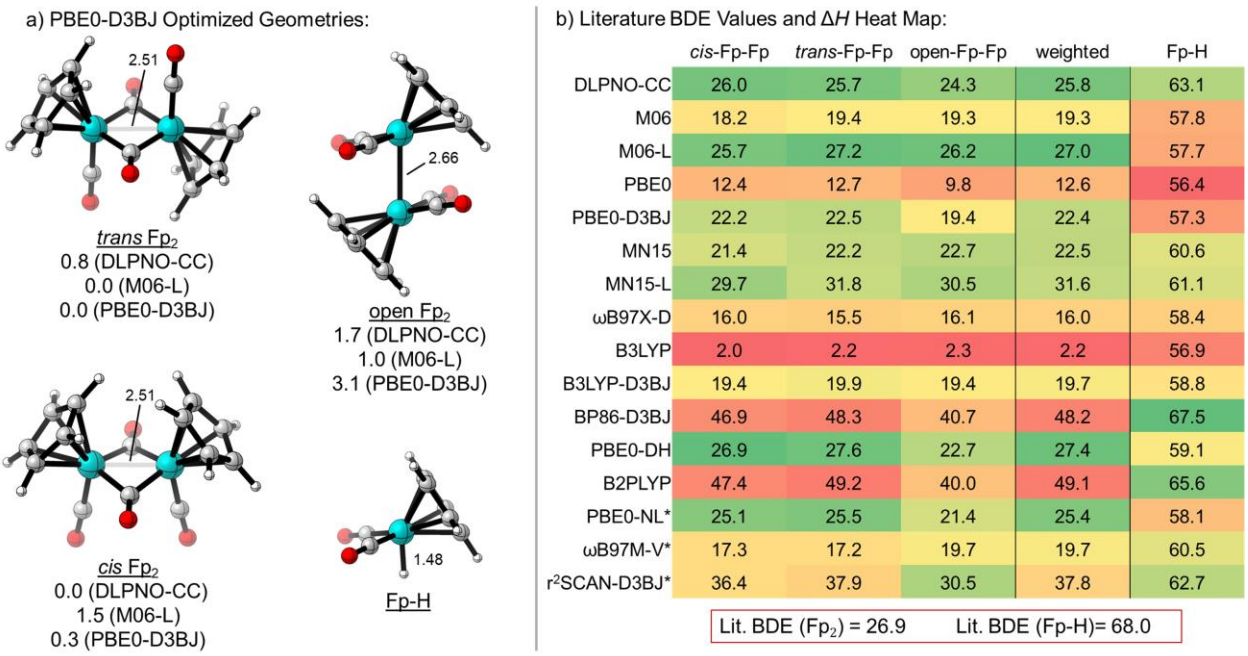

Figure 2. a) PBE0-D3BJ/def2-TZVP optimized geometries and their relative configuration enthalpies in the gas phase. b) Heat map showing the fragmentation enthalpy values for each fluxional Fp_2 isomer including the Boltzmann weighted deviations, and the Fp-H species. All enthalpies reported are in kcal/mol. *Indicates that the single point energy calculation was performed with ORCA.

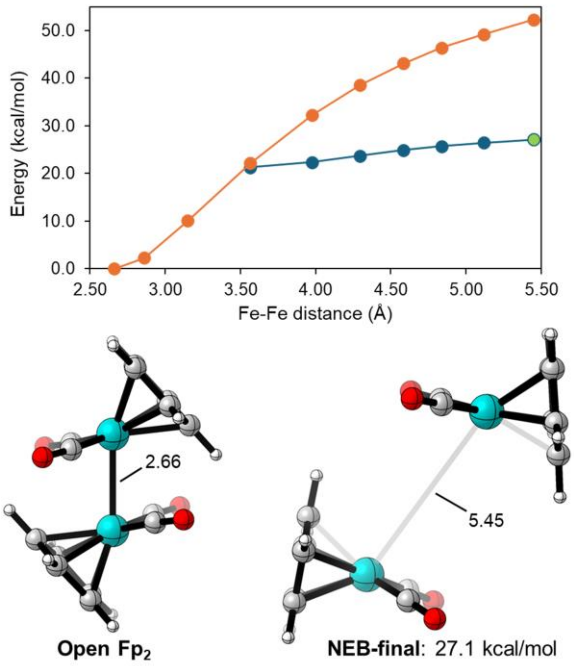

Figure 3. Nudged elastic band (NEB) calculations shown with open- (blue) and closed-shell (orange) electronic energies. The NEB calculation was performed at the M06-L(DEFGRID3)/def2-TZVP//M06-L/def2-SVP level of theory in the gas phase. All are energies reported are in kcal/mol.

We started our evaluation of DFT methods with PBE0 (which includes the D3BJ dispersion correction; labeled as PBE0-D3BJ in Figure 2) by calculating Fp_2 and the corresponding Fp• radical geometry (doublet spin state) and this gave an enthalpy change of 22.5 kcal/mol starting with the *trans* configuration and 22.2 kcal/mol starting with the *cis* configuration. This PBE0-D3BJ fragmentation energy is only too low by ~4 kcal/mol and this difference could be due to solvent effects not explicitly included in the calculation (see later discussion). Comparison of PBE0-D3BJ to PBE0 shows that without dispersion the error goes from reasonable to unacceptable at over 12 kcal/mol. A similar situation is found with B3LYP, which has an error of over 22 kcal/mol but inclusion of D3BJ dispersion provides and error of just over 5 kcal/mol. It should be noted that inclusion of dispersion with a functional does not always lead to accurate results. For example, BP86-D3BJ has an error of >16 kcal/mol. Figure 2 and the SI provides a detailed list of other density functionals used to evaluate the fragmentation energy of Fp_2. The most accurate method with consideration of the experimental error, which is a middle rung method, was M06-L,[45] which gave an energy of 27.2 kcal/mol for the *trans* configuration and 25.7 kcal/mol for the *cis* configuration. The table in Figure 2b also gives Boltzmann weighted fragmentation energy, and for M06-L this value is 27.0 kcal/mol.

In addition to checking the accuracy of lower rung methods we also wanted to extensively evaluate the highest DFT rung, which is generally considered to be double-hybrid methods. Surprisingly, checking the double-hybrid DFT methods showed highly inconsistent results with Fp_2 fragmentation energies varying from 26.9-53.9 kcal/mol. For example, while PBE0-DH gave a Boltzmann weighted fragmentation enthalpy of 27.4 kcal/mol the B2PLYP method, which is often used in computational studies of transition metal systems, gave a weighted bond enthalpy of 49.1 kcal/mol, which is a more than 20 kcal/mol error from experiment. We also evaluated the DLPNO-CCSD(T) method. The DLPNO-CCSD(T) fragmentation enthalpy starting from the *trans* configuration is 27.2 kcal/mol and the from the *cis* configuration is 28.0 kcal/mol, which are both close to the experimental value.

With M06-L and PBE0-D3BJ providing highly reasonable values for the Fp_2 fragmentation energy we wanted to evaluate the bonding changes that occur during the fragmentation process leading to Fp•. As previously noted, Hoffmann and coworkers reported an extensive extended Huckel orbital bonding analysis of the *trans* Fp_2 configuration that indicated no direct Fe-Fe covalent bond.[46] More recently, Mankad and coworkers reported experimental electron density analysis of *cis* and *trans* configurations along with QTAIM analysis of the electron densities and also found no evidence for a significant direct covalent Fe-Fe bonding.[41] We examined the ground state *trans* Fp_2 dimer using intrinsic bond orbitals (IBOs), which are shown in Figure 4.[27] This IBO analysis showed two σ-symmetry orbitals responsible for the 3-centered, 2-electron bonds around each Fe-(CO)-Fe moiety, two pseudo π-symmetry 3-centered, 2-electron bonds around each CO-Fe-CO moiety, and the unique 4-centered, 2-electron bond around the Fe-$(CO)_2$-Fe core. Overall, the IBOs are highly consistent with the Huckel-type orbitals previously presented by Hoffmann and coworkers.

Despite orbital bonding analysis suggesting no direct Fe-Fe covalent bond in *trans* Fp_2, Labinger has argued[47] that representing Fp_2 with a direct Fe-Fe covalent bond in the ground state hints that the fragmentation of Fp_2 will generate Fp•. This prompted us to evaluate the configurations and orbital bonding that occurs as Fp_2 fragments to Fp•. Figure 5a and 5b plot the enthalpy change of *trans* Fp_2 fragmentation as a function freezing the Fe-Fe and Fe-CO distances, which results in two slightly different fragmentation pathways. At each structure along this pathway, we evaluated the configuration. After only 0.2 Å Fe-Fe distance increase the structure changed to the open configuration, which is consistent with the relative energies of the *trans* and open configurations. We also used IBOs to track the pseudo π-symmetry orbital responsible for the unique 4-centered, 2-electron bond around the Fe-$(CO)_2$-Fe core that is responsible for the closed-shell electronic structure of *trans* Fp_2 (Figure 5c).[28] Consistent with the change from *trans* to open configurations with only slight increase in the Fe-Fe distance, the pseudo π-symmetry orbital changes to a σ-symmetry orbital indicative of a covalent Fe-Fe bond. This suggests that while there is no covalent Fe-Fe bond in the ground state, very early along the reaction pathway for fragmentation the Fe-Fe bond is established and then broken which provides the Fp radicals. Consistent

with this viewpoint, we located the *cis*-to-*trans* isomerization transition-state structure, and it has an enthalpy barrier of 10.5 kcal/mol, which is less than half that of the fragmentation energy.

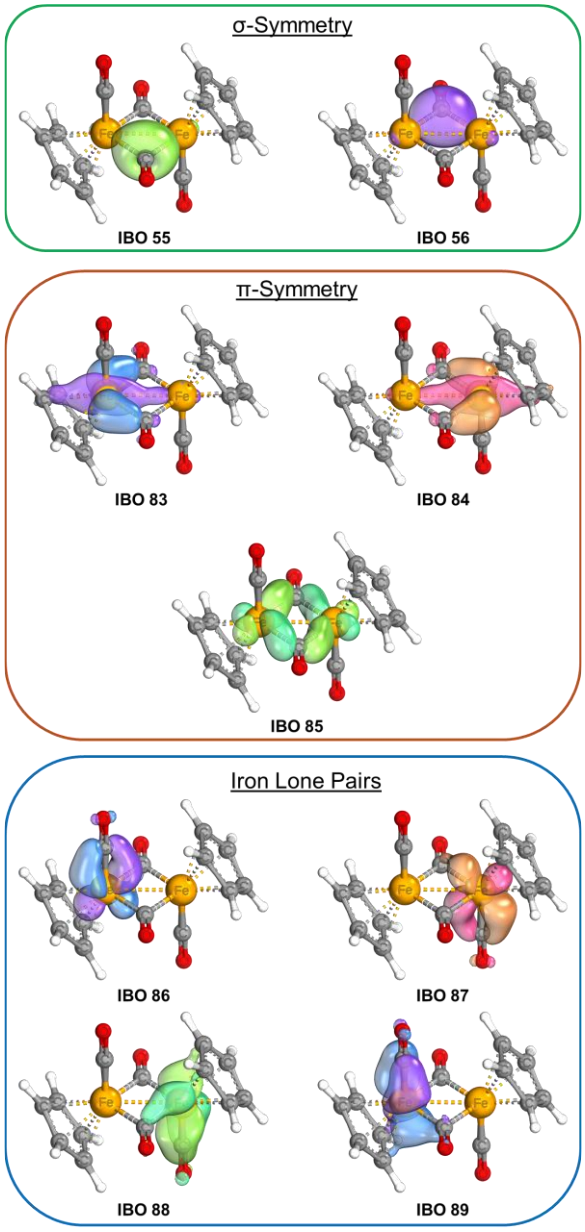

Figure 4. Intrinsic bonding orbitals (IBOs) of *trans* Fp_2 involving Fe electrons (14 electrons) and bridging carbonyl electrons (4 electrons).

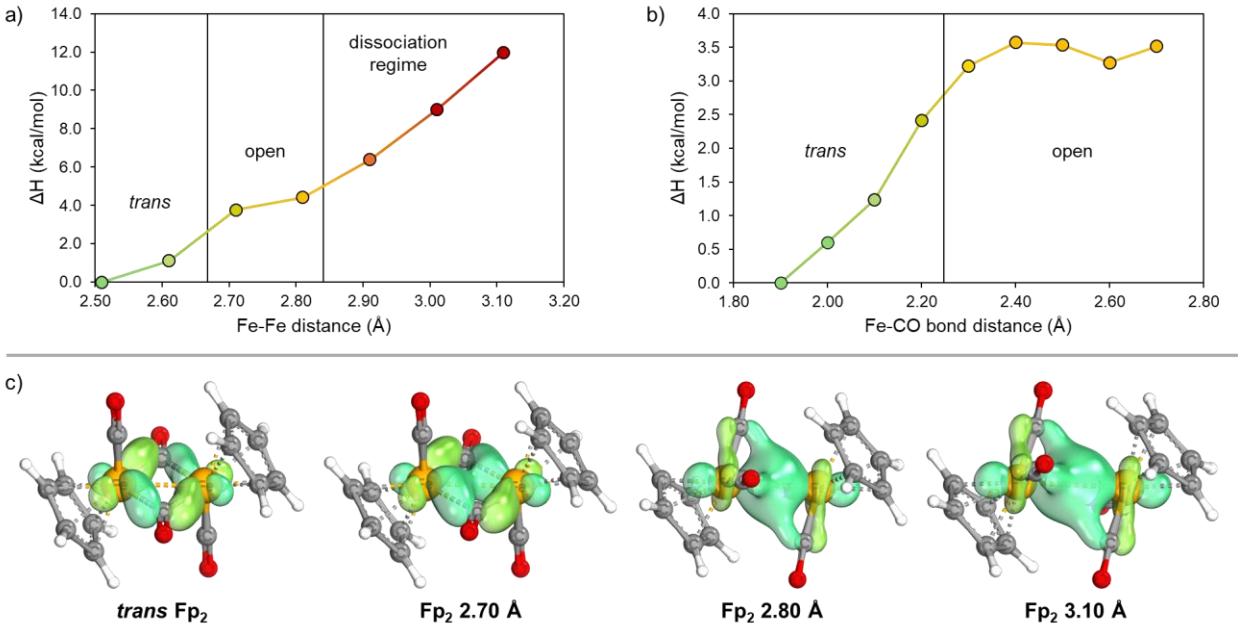

Figure 5. a) Fe-Fe distance reaction coordinate for Fp_2 fragmentation. After 0.2 Å of Fe-Fe distance displacement the *trans* configuration converts to the open configuration. b) Fe-CO distance reaction coordinate for Fp_2 fragmentation. c) Structures of the *trans*-Fp_2 with IBOs shown along the Fe-Fe distance reaction coordinate.

With the accuracy for Fp_2 fragmentation evaluated we wanted to then determine which DFT methods also provide accurate evaluation of generating Fp• from a different starting complex, specifically a mononuclear Fe complex. The most related mononuclear bond energy that has been experimentally measured is the Fe-H bond in Fp-H. This bond enthalpy was experimentally determined to be 68.0 kcal/mol by Lichtenberger and Norton who used pK_a values and oxidation potentials for Fp-H with multiple different bases in order to derive this energy value (taken to be enthalpy).[14] The Fp-H bond energy results in H• and Fp•, which is the same radical resulting from the Fp_2 fragmentation. Therefore, we began by examining the best performing DFT methods for Fp_2, which were PBE0-D3BJ and M06-L. These methods gave bond enthalpy values of 57.3 and 57.7 kcal/mol, respectively (Figure 2b). Both methods have a deviation from the experimental value by more than 10 kcal/mol. Perhaps surprisingly, despite the accuracy found for the Fp_2 system, evaluation of other lower rung and mid rung DFT methods showed a general pattern that methods that are accurate for the Fp_2 fragmentation energy struggle with the Fe-H bond and methods that are accurate for the Fe-H bond struggle with the Fp_2 energy. This suggests that there are likely different forms of inaccuracy and error cancellation in DFT methods applied to these two different types of bonding situations, despite them both having a common Fp• metalloradicaloid. However, it should be noted that this is not simply due to the unique delocalized bonding found in *cis* and *trans* Fp_2 because the energy of the open configuration that has a Fe-Fe bond gives highly similar results.

Similar to the lower and mid rung DFT methods, but exacerbated, the highest rung double-hybrid methods again shows that the accurate method for Fp_2 fails for the Fe-H bond and vice versus. For example, PBE-DH method deviates by over 8 kcal/mol for the Fe-H bond despite being close to the experimental accuracy for Fp_2. The B2PLYP method that was disastrously incorrect for Fp_2 shows a deviation of only 2.4 kcal/mol for the Fe-H bond. It is possible for these MP2-based methods that high spin intruder states may be responsible for the large swings in accuracy. In general, Hartree-Fock and MP2 methods struggle with bond dissociation energies due to spin contamination and symmetry problems arising in-part from mean-field Hartree-Fock orbitals, which appear even in the absence of transition metals, though there are methods such are orbital optimization and spin-component scaling that can alleviate these issues.[48] Indeed, in the calculation of 44 small molecule X-NO_2 bond energies, Liu et al.

found that MP2 was yielding huge positive deviations in energy,[49] which is the same type of deviation we observed with MP2 for Fp• radical with Fp_2. However, this organometallic case is likely more complex to properly capture the correct amount of dynamic correlation.[48, 50] In the case of DH-DFT multiple studies have previously cast doubt on the use of these methods for radicals and organometallic species.[50-54] In particular, Shee and coworkers showed DH-DFT and OO-MP2 methods underperform in several cases for strong-field metal-CO ligand bond dissociations energies, and there were deviations from experimental values between 5-35 kcal/mol.[50, 55] These errors were attributed overestimation of the MP2 component of the calculations.

We did the same dinuclear to mononuclear comparison with DLPNO-CCSD(T)//PBE0-D3BJ. While we were expecting DLPNO-CCSD(T) to give a chemically accurate bond energy (typically considered to be ± 1 kcal/mol) it did not. For Fp-H DLPNO-CCSD(T) provided a bond energy of 62.8 kcal/mol, which is 5.2 kcal/mol lower than experiment. This again means that highly accurate methods, even wavefunction based methods, for Fp_2 do not necessarily translate to high accuracy of a mononuclear bond energy. However, the deviation in mononuclear BDE accuracy for DLPNO-CCSD(T) compared to the lower rung DFT methods, such as M06-L, is much smaller at about 50%. Therefore, when possible, it would be important to compare DFT values to DLPNO-CCSD(T) values.

An often-neglected aspect of evaluating the accuracy of organometallic fragmentation/bond energies is the impact of solvent. For organic bond energies neglecting solvent energies can be reasonable since there is a small interaction energy between organic radicals and solvent. However, with transition metal systems there is the possibility that solvent can strongly interact with the metal center through unoccupied or partially occupied coordination sites, and we recently showed this can be a large effect in heterodinuclear bonds.[56] Therefore, we modeled the Fp_2 fragmentation energy by starting with Fp_2 and two explicit solvents and the conversion to (benzene)(Cp)$(CO)_2$Fp•. Figure 6 provides a comparison of gas phase, continuum solvent, and explicit solvent values for the bond dissociation enthalpy. Important for confirming the fragmentation energies previously described, the addition of explicit solvent had a very minor effect on energies. For example, for *trans*-Fp_2 explicit solvent changed the fragmentation enthalpy by less than 1 kcal/mol and this is consistent with a relatively weak interaction and long distance between benzene and Fp•. The inclusion of continuum/implicit solvent results in a small increase in the fragmentation enthalpy. The enthalpy increases by 1-3 kcal/mol depending on the Fp_2 configuration, and this suggests that continuum models may stabilize the Fp_2 complexes.

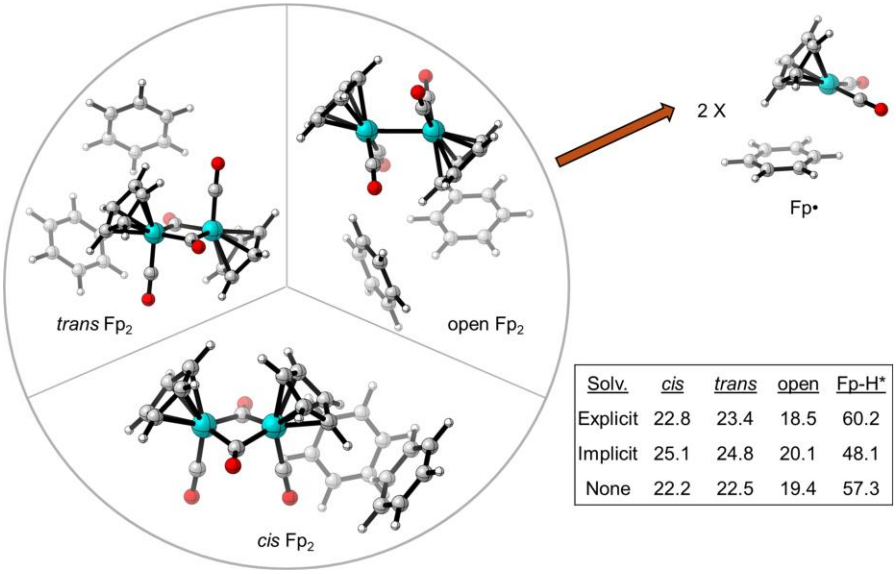

Solv.	*cis*	*trans*	open	Fp-H*
Explicit	22.8	23.4	18.5	60.2
Implicit	25.1	24.8	20.1	48.1
None	22.2	22.5	19.4	57.3

Figure 6. PBE0-D3BJ/def2-TZVP optimized geometries of explicitly solvated structures and table with bond dissociation enthalpies in the gas phase, explicit solvent, and continuum solvent (kcal/mol). Explicit

solvation geometries were optimized without continuum solvation. Implicit geometries were optimized with SMD continuum solvation for parameters with benzene.
*For Fp-H the implicit geometries were optimized with SMD solvation for parameters with MeCN and explicit solvation used MeCN molecules.

Conclusions

Dinuclear complexes with metal-metal bonds have emerged as unique catalysts and DFT methods remain the only practical way to evaluate reaction mechanisms. Therefore, in this work we evaluated the accuracy of DFT and coupled cluster methods for the Fe-Fe bond enthalpy of Fp_2 and the Fe-H bond in Fp-H. The Fe-H bond was evaluated because in many catalytic cycles dinuclear species evolve into mononuclear species, and this provides a comparison of dinuclear to mononuclear accuracy. DFT methods provided a surprising wide range of bond energies for Fp_2 and lower and mid rung DFT methods and coupled cluster methods performed well for this dinuclear bond energy. The best performing functional was M06-L. Interestingly, PBE0 and B3LYP functionals without dispersion show significant errors. However, dispersion does not guarantee accuracy, which was shown with the BP86 functional. The highest rung double-hybrid methods also had a large range in bond energies and the bond energy greatly depended on the amount of MP2 correlation energy included. For example, while PBE0-DH showed an accurate bond energy B2PLYP had an error of greater than 20 kcal/mol. For the Fe-H bond in Fp-H the lower and mid rung methods that worked well for the Fe-Fe bond showed significant error for the Fe-H bond. Double-hybrid methods unfortunately are only accurate for the Fe-H bond if they are very inaccurate for the Fe-Fe bond. Perhaps as expected, coupled cluster theory is not perfect, but it did provide reasonable accuracy for both dinuclear and mononuclear bond energies. Overall, this work indicates that for dinuclear catalysis that often toggles between dinuclear and mononuclear structures care must be taken to determine which DFT method is most accurate, and this selection should be based on properties of both dinuclear and mononuclear structures.

Supporting Information

Xyz coordinates, absolute energies, and additional calculation comparisons (MP2, FOD, and CASPT2).

Corresponding Author Information
***Daniel H. Ess** – *Department of Chemistry and Biochemistry, Brigham Young University, Provo, Utah 84604, United States*; Email: dhe@byu.edu

Authors
Kevin P. Quirion – *Department of Chemistry and Biochemistry, Brigham Young University, Provo, Utah 84604, United States*

Neal P. Mankad – *Department of Chemistry, University of Illinois, Chicago, IL 60607, United States*

Roushan Prakash Singh – *Department of Chemistry, University of Illinois, Chicago, IL 60607, United States*

Acknowledgments

The authors thank Brigham Young University and the Fulton Supercomputing Lab for computational resources. This work was primarily supported by the US National Science Foundation with the award CHE-2153215 (to DHE). This material is based upon work supported by the U.S. Department of Energy, Office of Science, Office of Basic Energy Sciences, under Grant DE-SC0021055 (to NPM).

References

(1) Jensen, K. P.; Roos, B. O.; Ryde, U. Performance of density functionals for first row transition metal systems. *The Journal of Chemical Physics* **2007**, *126* (1). DOI: 10.1063/1.2406071 (acccessed 2/13/2025).
(2) Moltved, K. A.; Kepp, K. P. Chemical Bond Energies of 3d Transition Metals Studied by Density Functional Theory. *Journal of Chemical Theory and Computation* **2018**, *14* (7), 3479-3492. DOI: 10.1021/acs.jctc.8b00143.
(3) Maurer, L. R.; Bursch, M.; Grimme, S.; Hansen, A. Assessing Density Functional Theory for Chemically Relevant Open-Shell Transition Metal Reactions. *Journal of Chemical Theory and Computation* **2021**, *17* (10), 6134-6151. DOI: 10.1021/acs.jctc.1c00659.
(4) Petrie, S.; Stranger, R. DFT and Metal−Metal Bonding: A Dys-Functional Treatment for Multiply Charged Complexes? *Inorganic Chemistry* **2004**, *43* (8), 2597-2610. DOI: 10.1021/ic034525e.
(5) Cotton, F. A.; Feng, X. Density Functional Theory Study of Transition-Metal Compounds Containing Metal−Metal Bonds. 1. Molecular Structures of Dinuclear Compounds by Complete Geometry Optimization. *Journal of the American Chemical Society* **1997**, *119* (32), 7514-7520. DOI: 10.1021/ja9705351.
(6) Cotton, F. A.; Feng, X. Density Functional Theory Study of Transition-Metal Compounds Containing Metal−Metal Bonds. 2. Molecular Structures and Vibrational Spectra of Dinuclear Tetracarboxylate Compounds of Molybdenum and Rhodium. *Journal of the American Chemical Society* **1998**, *120* (14), 3387-3397. DOI: 10.1021/ja9738236.
(7) Inatomi, T.; Koga, Y.; Matsubara, K. Dinuclear Nickel(I) and Palladium(I) Complexes for Highly Active Transformations of Organic Compounds. *Molecules* **2018**, *23* (1), 140.
(8) Wang, W.; Ji, C.-L.; Liu, K.; Zhao, C.-G.; Li, W.; Xie, J. Dinuclear gold catalysis. *Chemical Society Reviews* **2021**, *50* (3), 1874-1912, 10.1039/D0CS00254B. DOI: 10.1039/D0CS00254B.
(9) Zhong, D.-C.; Gong, Y.-N.; Zhang, C.; Lu, T.-B. Dinuclear metal synergistic catalysis for energy conversion. *Chemical Society Reviews* **2023**, *52* (9), 3170-3214, 10.1039/D2CS00368F. DOI: 10.1039/D2CS00368F.
(10) Kwon, D.-H.; Proctor, M.; Mendoza, S.; Uyeda, C.; Ess, D. H. Catalytic Dinuclear Nickel Spin Crossover Mechanism and Selectivity for Alkyne Cyclotrimerization. *ACS Catalysis* **2017**, *7* (7), 4796-4804. DOI: 10.1021/acscatal.7b00978.
(11) Kumawat, J.; Ess, D. H. On-Demand Metal-to-Metal Electron Donation during Zr–Ru Heterodinuclear-Catalyzed Amine–Borane Dehydrogenation. *ACS Catalysis* **2024**, *14* (22), 16947-16956. DOI: 10.1021/acscatal.4c03724.
(12) Coombs, J.; Perry, D.; Kwon, D.-H.; Thomas, C. M.; Ess, D. H. Why Two Metals Are Better Than One for Heterodinuclear Cobalt–Zirconium-Catalyzed Kumada Coupling. *Organometallics* **2018**, *37* (22), 4195-4203. DOI: 10.1021/acs.organomet.8b00449.
(13) Cutler, A. R.; Rosenblum, M. Kinetic determination of the metal・metal bond dissociation energy in bis(dicarbonyl η5-cyclopentadienyliron). *Journal of Organometallic Chemistry* **1976**, *120* (1), 87-96. DOI: https://doi.org/10.1016/S0022-328X(00)80407-6.
(14) Estes, D. P.; Vannucci, A. K.; Hall, A. R.; Lichtenberger, D. L.; Norton, J. R. Thermodynamics of the Metal–Hydrogen Bonds in (η5-C5H5)M(CO)2H (M = Fe, Ru, Os). *Organometallics* **2011**, *30* (12), 3444-3447. DOI: 10.1021/om2001519.
(15) *Gaussian 16 Rev. B.01*; Wallingford, CT, 2016. (accessed.

(16) Adamo, C.; Barone, V. Toward reliable density functional methods without adjustable parameters: The PBE0 model. *The Journal of Chemical Physics* **1999**, *110* (13), 6158-6170. DOI: 10.1063/1.478522 (acccessed 1/27/2025).
(17) Perdew, J. P.; Burke, K.; Ernzerhof, M. Generalized Gradient Approximation Made Simple. *Physical Review Letters* **1996**, *77* (18), 3865-3868. DOI: 10.1103/PhysRevLett.77.3865.
(18) Weigend, F.; Ahlrichs, R. Balanced basis sets of split valence, triple zeta valence and quadruple zeta valence quality for H to Rn: Design and assessment of accuracy. *Physical Chemistry Chemical Physics* **2005**, *7* (18), 3297-3305, 10.1039/B508541A. DOI: 10.1039/B508541A.
(19) Grimme, S. Semiempirical GGA-type density functional constructed with a long-range dispersion correction. *Journal of Computational Chemistry* **2006**, *27* (15), 1787-1799. DOI: https://doi.org/10.1002/jcc.20495 (acccessed 2025/01/27).
(20) Grimme, S.; Ehrlich, S.; Goerigk, L. Effect of the damping function in dispersion corrected density functional theory. *Journal of Computational Chemistry* **2011**, *32* (7), 1456-1465. DOI: https://doi.org/10.1002/jcc.21759 (acccessed 2025/01/27).
(21) Marenich, A. V.; Cramer, C. J.; Truhlar, D. G. Universal Solvation Model Based on Solute Electron Density and on a Continuum Model of the Solvent Defined by the Bulk Dielectric Constant and Atomic Surface Tensions. *The Journal of Physical Chemistry B* **2009**, *113* (18), 6378-6396. DOI: 10.1021/jp810292n.
(22) Zhao, Y.; Truhlar, D. G. A new local density functional for main-group thermochemistry, transition metal bonding, thermochemical kinetics, and noncovalent interactions. *The Journal of Chemical Physics* **2006**, *125* (19), 194101. DOI: 10.1063/1.2370993 (acccessed 1/27/2025).
(23) Brémond, E.; Adamo, C. Seeking for parameter-free double-hybrid functionals: The PBE0-DH model. *The Journal of Chemical Physics* **2011**, *135* (2), 024106. DOI: 10.1063/1.3604569 (acccessed 1/27/2025).
(24) Neese, F. The ORCA program system. *WIREs Computational Molecular Science* **2012**, *2* (1), 73-78. DOI: https://doi.org/10.1002/wcms.81.
(25) Purvis, G. D., III; Bartlett, R. J. A full coupled-cluster singles and doubles model: The inclusion of disconnected triples. *The Journal of Chemical Physics* **1982**, *76* (4), 1910-1918. DOI: 10.1063/1.443164 (acccessed 1/27/2025).
(26) Riplinger, C.; Pinski, P.; Becker, U.; Valeev, E. F.; Neese, F. Sparse maps—A systematic infrastructure for reduced-scaling electronic structure methods. II. Linear scaling domain based pair natural orbital coupled cluster theory. *The Journal of Chemical Physics* **2016**, *144* (2), 024109. DOI: 10.1063/1.4939030 (acccessed 1/27/2025).
(27) Knizia, G. Intrinsic Atomic Orbitals: An Unbiased Bridge between Quantum Theory and Chemical Concepts. *Journal of Chemical Theory and Computation* **2013**, *9* (11), 4834-4843. DOI: 10.1021/ct400687b.
(28) Knizia, G.; Klein, J. E. M. N. Electron Flow in Reaction Mechanisms—Revealed from First Principles. *Angewandte Chemie International Edition* **2015**, *54* (18), 5518-5522. DOI: https://doi.org/10.1002/anie.201410637 (acccessed 2025/05/20).
(29) Burke, K. Perspective on density functional theory. *The Journal of Chemical Physics* **2012**, *136* (15). DOI: 10.1063/1.4704546 (acccessed 4/16/2025).

(30) Rappoport, D.; Crawford, N. R. M.; Furche, F.; Burke, K. Approximate Density Functionals: Which Should I Choose? In *Encyclopedia of Inorganic Chemistry*, 2005.
(31) Harvey, J. N. On the accuracy of density functional theory in transition metal chemistry. *Annual Reports Section "C" (Physical Chemistry)* **2006**, *102* (0), 203-226, 10.1039/B419105F. DOI: 10.1039/B419105F.
(32) Sinhababu, S.; Singh, R. P.; Radzhabov, M. R.; Kumawat, J.; Ess, D. H.; Mankad, N. P. Coordination-induced O-H/N-H bond weakening by a redox non-innocent, aluminum-containing radical. *Nature Communications* **2024**, *15* (1), 1315. DOI: 10.1038/s41467-024-45721-1.
(33) Tsuji, J.; Mori, Y. Organic Syntheses by Means of Metal Complexes. II. Oxo Reaction Catalyzed by Cyclopentadienyliron Dicarbonyl Dimer. *Bulletin of the Chemical Society of Japan* **2006**, *42* (2), 527-529. DOI: 10.1246/bcsj.42.527 (acccessed 4/18/2025).
(34) Yang, F.; Yu, P.; Zhao, J.; Shi, J.; Wang, J. Ultrafast vibrational and structural dynamics of dimeric cyclopentadienyliron dicarbonyl examined by infrared spectroscopy. *Physical Chemistry Chemical Physics* **2015**, *17* (22), 14542-14550, 10.1039/C5CP00965K. DOI: 10.1039/C5CP00965K.
(35) Hooker, R. H.; Mahmoud, K. A.; Rest, A. J. Spectroscopic evidence for the formation of tri-μ-carbonyl-bis-[(η5-cyclopentadienyl)iron] on photolysis of bis[(dicarbonyl)(η5-cyclopentadienyl)iron] in low temperature matrices. *Journal of the Chemical Society, Chemical Communications* **1983**, (18), 1022-1024, 10.1039/C39830001022. DOI: 10.1039/C39830001022.
(36) Dalton, E. F.; Ching, S.; Murray, R. W. Cryoelectrochemical study of the cleavage of radical anions of diiron and diruthenium carbonyl dimers. *Inorganic Chemistry* **1991**, *30* (12), 2642-2648. DOI: 10.1021/ic00012a015.
(37) Shackleton, T. A.; Mackie, S. C.; Fergusson, S. B.; Johnston, L. J.; Baird, M. C. The chemistry of (.eta.5-cyclopentadienyl)dicarbonyliron hydride revisited. *Organometallics* **1990**, *9* (8), 2248-2253. DOI: 10.1021/om00158a023.
(38) Angerer, W.; Fiederling, K.; Grötsch, G.; Malisch, W. Phosphonium-metallate, V. Carbonyl(hydrido)(η5-pentamethylcyclopentadienyl) (trimethyl-phosphan)eisen(II): Darstellung und Umsetzung mit Trimethyl(methylen)phosphoran. *Chemische Berichte* **1983**, *116* (12), 3947-3950. DOI: https://doi.org/10.1002/cber.19831161217.
(39) Bryan, R. F.; Greene, P. T. Metal–metal bonding in co-ordination complexes. Part IX. Crystal structure of trans-di-μ-carbonyl-dicarbonyldi-π-cyclopentadienyldi-iron (Fe–Fe), a redetermination. *Journal of the Chemical Society A: Inorganic, Physical, Theoretical* **1970**, (0), 3064-3068, 10.1039/J19700003064. DOI: 10.1039/J19700003064.
(40) Mills, O. Studies of some carbon compounds of the transition metals. I. The crystal structure of dicyclopentadienyldiiron tetracarbonyl. *Acta Crystallographica* **1958**, *11* (9), 620-623. DOI: doi:10.1107/S0365110X58001663.
(41) Yan, C.; Radzhabov, M. R.; Chang, T.; Chen, Y.-S.; Mankad, N. P. Comprehensive Re-examination of Intermetallic Charge Density for the Metal Carbonyl Dimers Mn2(CO)10 and [(η5-C5H5)Fe(CO)2]2. *Inorganic Chemistry* **2025**, *64* (9), 4514-4523. DOI: 10.1021/acs.inorgchem.4c05427.
(42) Bryan, R. F.; Greene, P. T.; Newlands, M. J.; Field, D. S. Metal–metal bonding in co-ordination complexes. Part X. Preparation, spectroscopic properties, and crystal structure

of the cis-isomer of di-μ-carbonyl-dicarbonyldi-π-cyclopentadienyldi-iron (Fe–Fe). *Journal of the Chemical Society A: Inorganic, Physical, Theoretical* **1970**, (0), 3068-3074, 10.1039/J19700003068. DOI: 10.1039/J19700003068.
(43) Harris, D. C.; Rosenberg, E.; Roberts, J. D. Carbon-13 nuclear magnetic resonance spectra and mechanism of bridge–terminal carbonyl exchange in di-μ-carbonyl-bis[carbonyl(η-cyclopentadienyl)iron](Fe–Fe)[{(η-C5H5)Fe(CO)2}2]; cd-di-μ-carbonyl-f-carbonyl-ae-di(η-cyclopentadienyl)-b-(triethyl -phosphite)di-iron(Fe–Fe)[(η-C5H5)2Fe2(CO)3P(OEt)3], and some related complexes. *Journal of the Chemical Society, Dalton Transactions* **1974**, (22), 2398-2403, 10.1039/DT9740002398. DOI: 10.1039/DT9740002398.
(44) Day, G. M. Current approaches to predicting molecular organic crystal structures. *Crystallography Reviews* **2011**, *17* (1), 3-52. DOI: 10.1080/0889311X.2010.517526.
(45) Shil, S.; Bhattacharya, D.; Sarkar, S.; Misra, A. Performance of the Widely Used Minnesota Density Functionals for the Prediction of Heat of Formations, Ionization Potentials of Some Benchmarked First Row Transition Metal Complexes. *The Journal of Physical Chemistry A* **2013**, *117* (23), 4945-4955. DOI: 10.1021/jp400397r.
(46) Jemmis, E. D.; Pinhas, A. R.; Hoffmann, R. Cp2M2(CO)4 - quadruply bridging, doubly bridging, semibridging, or nonbridging? *Journal of the American Chemical Society* **1980**, *102* (8), 2576-2585. DOI: 10.1021/ja00528a010.
(47) Labinger, J. A. Does cyclopentadienyl iron dicarbonyl dimer have a metal–metal bond? Who's asking? *Inorganica Chimica Acta* **2015**, *424*, 14-19. DOI: https://doi.org/10.1016/j.ica.2014.04.022.
(48) Cremer, D. Møller–Plesset perturbation theory: from small molecule methods to methods for thousands of atoms. *WIREs Computational Molecular Science* **2011**, *1* (4), 509-530. DOI: https://doi.org/10.1002/wcms.58.
(49) Liu, J.; He, X.; Xiong, Y.; Nie, F.; Zhang, C. Benchmark calculations and error cancelations for bond dissociation enthalpies of X–NO2. *Defence Technology* **2023**, *22*, 144-155. DOI: https://doi.org/10.1016/j.dt.2021.11.014.
(50) Shee, J.; Loipersberger, M.; Hait, D.; Lee, J.; Head-Gordon, M. Revealing the nature of electron correlation in transition metal complexes with symmetry breaking and chemical intuition. *The Journal of Chemical Physics* **2021**, *154* (19), 194109. DOI: 10.1063/5.0047386 (acccessed 1/27/2025).
(51) Bursch, M.; Mewes, J.-M.; Hansen, A.; Grimme, S. Best-Practice DFT Protocols for Basic Molecular Computational Chemistry. *Angewandte Chemie International Edition* **2022**, *61* (42), e202205735. DOI: https://doi.org/10.1002/anie.202205735.
(52) Goerigk, L.; Grimme, S. Double-hybrid density functionals. *WIREs Computational Molecular Science* **2014**, *4* (6), 576-600. DOI: https://doi.org/10.1002/wcms.1193 (acccessed 2025/01/26).
(53) Martin, J. M. L.; Santra, G. Empirical Double-Hybrid Density Functional Theory: A 'Third Way' in Between WFT and DFT. *Israel Journal of Chemistry* **2020**, *60* (8-9), 787-804. DOI: https://doi.org/10.1002/ijch.201900114 (acccessed 2025/01/26).
(54) Sancho-García, J. C.; Adamo, C. Double-hybrid density functionals: merging wavefunction and density approaches to get the best of both worlds. *Physical Chemistry*

Chemical Physics **2013**, *15* (35), 14581-14594, 10.1039/C3CP50907A. DOI: 10.1039/C3CP50907A.
(55) Rudshteyn, B.; Coskun, D.; Weber, J. L.; Arthur, E. J.; Zhang, S.; Reichman, D. R.; Friesner, R. A.; Shee, J. Predicting Ligand-Dissociation Energies of 3d Coordination Complexes with Auxiliary-Field Quantum Monte Carlo. *Journal of Chemical Theory and Computation* **2020**, *16* (5), 3041-3054. DOI: 10.1021/acs.jctc.0c00070.
(56) Singh, R. P.; Quirion, K. P.; Telser, J.; Ess, D. H.; Mankad, N. P. Cooperative Heterobimetallic CO2 Activation Involving a Mononuclear Aluminum(II) Intermediate. *Journal of the American Chemical Society* **2025**, *147* (15), 12715-12721. DOI: 10.1021/jacs.5c00944.

TOC graphic

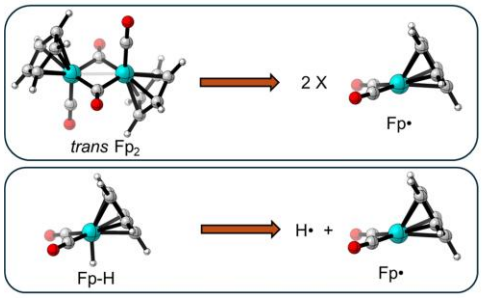

Fragmentation energy of Fp dimer and Fp-H

Method	Fp_2 accuracy	Fp-H accuracy
Lit. value	✓	✓
DLPNO-CC	✓	~
M06-L	✓	✗
MN15-L	~	~
PBE0-D3BJ	~	✗
PBE0-DH	✓	✗
B2PLYP	✗	✓